Femtosecond autocorrelator based on a swinging birefringent plate

S M Kobtsev, S V Smirnov, S V Kukarin, V B Sorokin

Abstract. **A new scheme of an interferometric scanning autocorrelator for measuring ultrashort light pulse durations in the femtosecond and subpicosecond ranges is considered. The distinguishing features of this scheme are its compact structure and a very simple adjustment. A variable time delay of ultrashort light pulse components is produced by a swinging birefringent plate made of a uniaxial crystal. Analytic expressions are obtained for the width of the scanning range and an optimal orientation of the optical axis of the crystal. The effect of disbalance in the intensities of waves that have propagated different optical paths on the form of the autocorrelation function (ACF) is analysed numerically. An experimental ACF for titanium-sapphire laser pulses of duration ∼ 25 fs is presented.**

Keywords: *autocorrelator, ultrashort pulses, birefringent crystal.*

1. Introduction

Autocorrelation methods are among the most important sources of information about the parameters of ultrashort laser pulses. The autocorrelation functions (ACFs) being recorded make it possible to determine the pulse duration and to analyse their temporal structure, including phase modulation parameters (of chirp) in the case of a symmetric pulse shape [1–3]. A large number of scanning autocorrelators based on the Michelson interferometer and intended for investigating ultrashort pulses with a relatively high pulse repetition rate have been designed and studied to data.

These autocorrelators differ mainly in the method of producing a variable optical delay of the ultrashort pulse in one of the arms of the interferometer and in the system of ACF recording. The variable optical delay is produced in autocorrelators based on the Michelson interferometer by a linear displacement [4–6] or rotation [7, 8] of a corner reflector, rotation (swinging) of a two-mirror periscope [9–11], or rotation of a reflector of special shape [12]. The interference pattern of the ACF being recorded provides

S M Kobtsev, S V Smirnov, S V Kukarin, V B Sorokin Novosibirsk State University, ul. Pirogova 2, 630090 Novosibirsk, Russia; e-mail: kobtsev@lab.nsu.ru

time marks that can be used for an easy and quite accurate calibration of the ACF time scale.

One of drawbacks of autocorrelators in which the time scan is performed by varying the length of one of the arms of the Michelson interferometer, is the need for their careful adjustment: the lengths L of the Michelson interferometer arms in the middle of the scanning range must be equal with an error of the order $c\Delta\tau$, where c is the velocity of light and $\Delta\tau$ is the duration of the pulse being studied. For pulses of durations 100 and 10 fs, this corresponds to the accuracy 30 and 3 μm, respectively. The requirement of equality of the Michelson interferometer arms can be alleviated by increasing the scan range. In this case, the error in the initial equalisation of the length of the arms will simply result in the fact that the difference in the optical paths will be equal to zero not in the middle of the scan range. To determine the ACF in this case, it is sufficient to satisfy the condition of equality of the arms of the Michelson interferometer within an accuracy of the order of $c\Delta T$, where ΔT is the scan range.

Therefore, an increase in the scan range of the autocorrelator simplifies its adjustment, but gives rise to another problem related to the maladjustment of the Michelson interferometer during scanning. This maladjustment is manifested at least in the form of an additional (spurious) amplitude modulation of the ACF, and at the most in the absence of interference between light beams emerging from different arms of the Michelson interferometer. Moreover, the ultrashort pulses may be distorted in the Michelson interferometer due to dispersion of the reflective coatings of the mirror and the 'transmission' optical elements (beamsplitter and retroreflecting prism), as well as due to the asymmetry of the interferometer configuration [13].

The drawbacks of the existing autocorrelators based on the Michelson interferometer stimulated the quest for new autocorrelating devices for ultrashort-pulse measurements. An interference scanning autocorrelator of an entirely different configuration (using a Wollaston prism) was proposed in Refs [14, 15]. The time delay between the ordinary and extraordinary waves of the input pulse can be varied by displacing the Wollaston prism in a direction perpendicular to the incident beam. Autocorrelators of such a construction virtually do not require any adjustment, but they can distort the initial ultrashort pulse, and hence the ACF, because of a relatively large thickness of the Wollaston prisms being used, as well as due to a nonuniformity in the optical delay over the beam cross section arising in the plane of connection of trigonal prisms.

In this work, we consider a new scheme of a scanning femtosecond autocorrelator [16] which practically does not
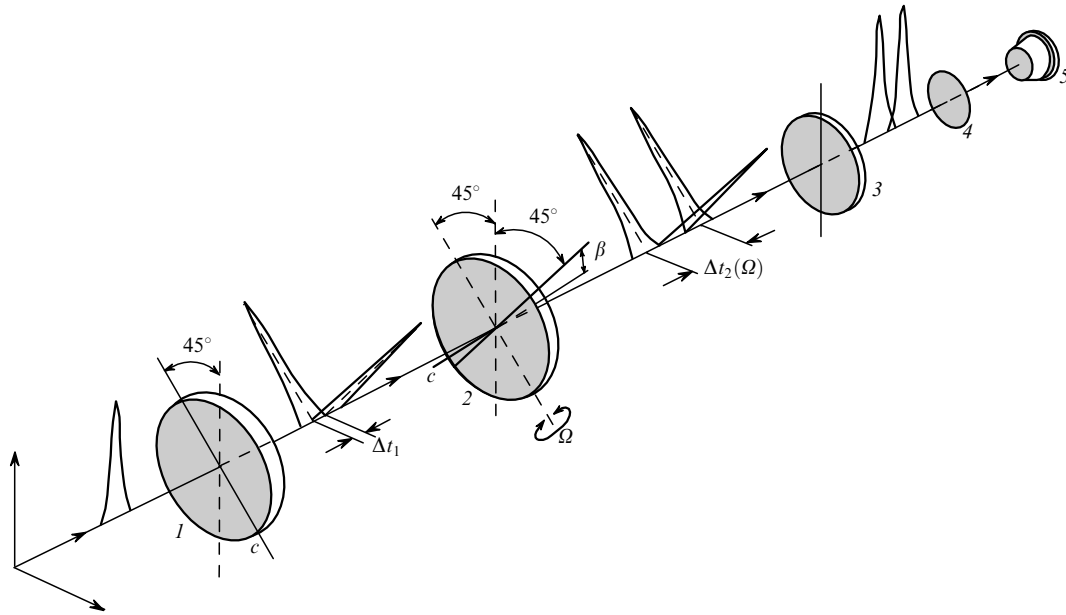
Figure 1. Schematic of a scanning autocorrelator based on a swinging birefringent plate: (*1*) fixed birefringent plate; (*2*) swinging birefringent plate; (*3*) polarisation filter; (*4*) lens; (*5*) nonlinear photodetector; (c) optical axis; (*β*) angle between the optical axis and the plate surface; (*Ω*) angle of deviation of plate (*2*) from the axis lying in the plane of the plate and perpendicular to the projection of the optical axis on the plate surface; Δt_1 and $\Delta t_2(\Omega)/2$ are time delays between the ordinary and extraordinary components of the pulse after plates (*1*) and (*2*), respectively.

require any adjustment, can be fabricated quite easily, and is capable of recording ACFs at a lower level of distortion of the temporal structure of the initial ultrashort pulse.

2. Schematic of the autocorrelator

Fig. 1 shows the schematic of the autocorrelator. A laser pulse passes through the birefringent plate (*1*) whose optical axis is parallel to its surface and forms an angle of $45°$ with the polarisation plane of the incident beam. This leads to the formation of ordinary and extraordinary components of the initial pulse, which are polarised in mutually orthogonal planes and are separated by a time interval Δt_1.

These components then pass through the birefringent plate (*2*) whose optical axis forms an angle β with its surface, and the projection of the optical axis on the surface of the plate is orthogonal to the optical axis of plate (*1*). The component of the initial pulse that passed through plate (*1*) as an ordinary wave, will pass through plate (*2*) as an extraordinary wave, and vice versa, so that for an appropriate choice of the parameters of plates (*1*) and (*2*), the total time delay Δt between the components of the initial pulse after their passing through plates (*1*) and (*2*) may be equal to zero and will reverse its sign upon a certain variation of the orientation of plate (*2*) (for example, during its swinging). Thus, a smooth alternating delay of the initial pulse components relative to each other can be achieved in this scheme.

After this, the components of the pulse pass through a polarisation filter (*3*), and their superposition is focused by lens (*4*) on a nonlinear photodetector (*5*) whose electric response is proportional to the square of the intensity of the ultrashort pulse being detected. A light emitting diode was used as a nonlinear photodetector [14, 17]. The main requirement imposed on the LED is that its band gap should be larger than that of the input photon. In this case, the transition of an electron to the conduction band occurs upon a simultaneous absorption of two photons. This provides the required nonlinear electric response of photodetector (*5*) [18].

As nonlinear photodetectors in autocorrelators, light-emitting diodes or photodiodes [19 – 21], laser diodes [22], semiconducting fibres [23], or other devices [24, 25] can be used. Unlike the traditional nonlinear crystal – linear photodetector pairs used earlier for recording ACFs, the above-mentioned nonlinear photodetectors provide a nonlinear electric response over a wider spectral range without any need for their adjustment (as long as the condition $E/2 < h\nu < E$ is satisfied, where E is the band gap and $h\nu$ is the photon energy), do not distort the temporal structure of the ultrashort pulse during recording (a nonlinear crystal may distort the temporal profile of the ultrashort pulse when phase matching or spectral matching are inadequate [10], etc.), are more sensitive (with a nonlinear response $\sim 10^{-2} - 10^{-5}$ nA mW^{-2} [18]), and have a longer service life (compared to nonlinear crystals), being relatively cheap. In the autocorrelator being considered here, we used an AL307 light-emitting diode as a nonlinear photodetector in the spectral range $700 - 1000$ nm; however, other nonlinear photodetectors can also be used.

3. Calculation of parameters of a swinging birefringent plate

Consider the propagation of a light beam through a tilted birefringent plate (Fig. 2). The optical delay between the ordinary and extraordinary waves after the birefringent plate is the sum of the phase differences acquired inside the plate ($\delta\varphi_{in}$) and outside it ($\delta\varphi_{ext}$):
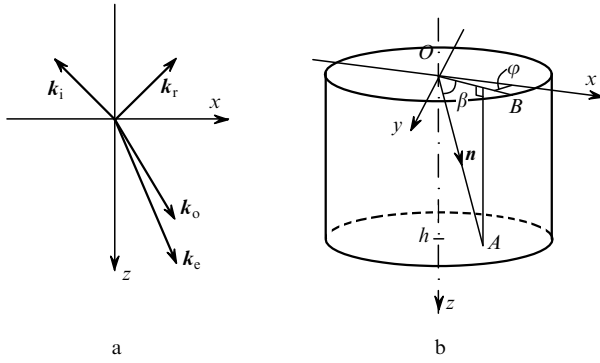
Figure 2. Propagation of a light beam through a tilted birefringent plate: (a) in the reference frame used by us (the x-axis is directed along the normal to the plate, the xz plane is the incidence plane containing the wave vectors), and (b) in the birefringent plate geometry (OA is the optical axis, OB is its projection on the plate surface, $\boldsymbol{n}$ is a unit vector directed along the optical axis, h is the plate thickness, β is the angle between the optical axis and the plate surface, φ is the angle between the projection of the optical axis on the plate surface and the incidence plane xz.

$$\delta\varphi = \delta\varphi_{\text{in}} + \delta\varphi_{\text{ext}} = \left(\frac{k_o S_o}{S_{oz}} - \frac{k_e S_e}{S_{ez}}\right)h$$

$$+ \left(\frac{k_i S_e}{S_{ez}} - \frac{k_i S_o}{S_{oz}}\right)h, \qquad (1)$$

where $\boldsymbol{k}_i$, $\boldsymbol{k}_r$, $\boldsymbol{k}_o$ and $\boldsymbol{k}_e$ are the wave vectors of the incident, reflected, ordinary and extraordinary waves, respectively; $\boldsymbol{S}_o$, $\boldsymbol{S}_e$ are the Poynting vectors; S_{oz}, S_{ez} are their projections on the z-axis; and h is the plate thickness.

By transforming Eqn (1) using expressions for k_{oz} and k_{ez} obtained from the solution of the Fresnel equation [26], and the dependences between the angles characterising the position of the optical axis of the birefringent plate [27], we arrive at the following expression for the time delay between the ordinary and extraordinary waves emerging from the tilted birefringent plate:

$$\delta t = \frac{h}{c}\left\{(n_o^2 - \sin^2 i)^{1/2} + \frac{\delta_n \sin\beta\cos\beta\sin i\cos\varphi}{\delta_n\sin^2\beta + n_e^{-2}}\right.$$

$$- \frac{1}{\delta_n\sin^2\beta + n_e^{-2}}\left[\delta_n^2\sin^2\beta\cos^2\beta\sin^2 i\cos^2\varphi \right. \qquad (2)$$

$$\left.\left. - \left(\delta_n\sin^2\beta + n_e^{-2}\right)\left(\delta_n\cos^2\beta\sin^2 i\cos^2\varphi + n_e^{-2}\sin^2 i - 1\right)\right]^{1/2}\right\},$$

where i is the angle of incidence; β is the angle between the optical axis and the plate surface; φ is the angle between the x-axis and the projection of the optical axis on the plate surface (Fig. 2b); and $\delta_n = n_o^{-2} - n_e^{-2}$.

For the birefringent plate (2) (Fig. 1) swinging with the angular amplitude Ω_{max} (so that the angle of incidence i varies from $-\Omega_{\text{max}}$ to Ω_{max}), the range of optical delay variation is determined by the second term in (2) since this is the only term containing a linear dependence on the angle i (the terms not containing $\sin i$ do not affect the width of the variation range δt, while higher even-order terms can be neglected if a coefficient at $\sin i$ is large, as is indeed the case). In this case, we obtain

$$\delta t_{\text{max}} - \delta t_{\text{min}} = \left|2\frac{h}{c}\frac{\delta_n\sin\beta\cos\beta\cos\varphi}{\delta_n\sin^2\beta + n_e^{-2}}\sin\Omega_{\text{max}}\right|. \qquad (3)$$

4. Optimisation of the parameters of birefringent plates of the autocorrelator

To extend the scan range defined by Eqn (3), it is necessary, first, to select a material with the highest value of $|\delta_n|$ for preparing the birefringent plate and, second, to choose an appropriate orientation of the optical axis of the birefringent plate and the axis of its swinging (angles β and φ in Fig. 2b). The angle φ should be equal to zero, i.e., the optical axis of the crystal should lie in the plane of incidence. The optimal value of the angle β between the optical axis and the surface of plate (2) in Fig. 1 is obtained by equating to zero the derivative of expression (3) with respect to β:

$$\beta_{\text{opt}} = \arcsin\left(\frac{n_o^2}{n_o^2 + n_e^2}\right)^{1/2}. \qquad (4)$$

By substituting the optimal values of the angles β and φ into expression (3), we obtain

$$\delta t_{\text{max}} - \delta t_{\text{min}} = \frac{h}{c}\frac{|n_o^2 - n_e^2|}{n_o n_e}\sin\Omega_{\text{max}}. \qquad (5)$$

It follows from Eqn (2) that for a fixed birefringent plate (1) of thickness h_1 for $i = 0$ and $\beta = 0$ (the light beam is incident along the normal and the optical axis lies in the plane of the plate), the optical delay Δt_1 has the form

$$\delta t_1 = \frac{h_1}{c}(n_o - n_e). \qquad (6)$$

To record the ACF in the limits symmetric in time (by neglecting the nonlinearity in the dependence of δt on the tilt angle Ω), the thickness h_1 of the fixed birefringent plate (1) must be chosen in such a way that the optical delay created by it is equal to the optical delay in plate (2) for $\Omega = 0$. For $i = 0$, we obtain from Eqns (6) and (2):

$$h_1 = \frac{h}{n_o - n_e}\left[n_o - \left(\frac{n_o^2 + n_e^2}{2}\right)^{1/2}\right] \approx \left(\frac{1}{2} - \frac{1}{8}\frac{n_o - n_e}{n_e}\right). \qquad (7)$$

Table 1 shows the optimal values of the angle β and the corresponding width of the scan range δt for plates made of uniaxial crystals of calcite ($CaCO_3$), yttrium vanadate (YVO_4), and rutile (TiO_2), which are characterised by a comparatively strong birefringence. The data were calculated as a result of computations for plates of thickness 1 mm (plate 2) for $\Omega_{\text{max}} = 15°$ and a wavelength of 800 nm. The corresponding thickness h_1 of the fixed plate (1), obtained from Eqn (7), is also presented in the table.

The uniaxial crystals under study have wide transparency regions covering a part of the visible spectrum

Table 1.

Plate material	n_o	n_e	δ_n	$\beta_{\text{opt}}/°$	$\delta t/\text{fs}$	h_1/mm
Calcite, ($CaCO_3$)	1.649	1.482	−0.0876	48.1	184.6	0.46
Yttrium vanadate (YVO_4)	1.972	2.186	0.0479	42.1	178.1	0.51
Rutile (TiO_2)	2.520	2.792	0.0292	42.1	177.2	0.51

(500–800 nm) and the near IR region (800–2000 nm) where many ultrashort-pulse lasers emit (Ti : sapphire, Cr : LiSAF, Cr/Yb/Nd : YAG, Cr : forsterite, Nd : YVO$_4$, Yb : YCOB/GdCOB and Er : Yb lasers, as well as semi-conductor and other lasers).

The width of the scan range, which is determined by Eqn (5), can be extended by increasing the plate thickness h and the angular amplitude Ω_{max} of its swing, but the following circumstances should be taken into account. To minimise the dispersion spread of input pulses during their passage through the plates, it is necessary to use plates with the smallest thickness. Their thickness should provide the scan range width at least of the order of the input pulse duration, but the ratio $\delta t_{max}/\Delta\tau$ should not be increased without need because of the possible dispersion spread of the input pulses.

The use of a sufficiently large angular amplitude of swinging of the plate leads to a considerable nonlinearity in the dependence of the optical delay on the incidence angle, as well as to a disbalance in the intensities of waves propagating through the swinging birefringent plate. The disbalance in the wave intensities is because the angle β is not zero. Fig. 3 shows the dependences of the intensities of waves on the angle Ω after their passage through a polarisation filter. These dependences are obtained by numerically solving the Fresnel problem on the propagation of a monochromatic wave through calcite plates of the autocorrelator.
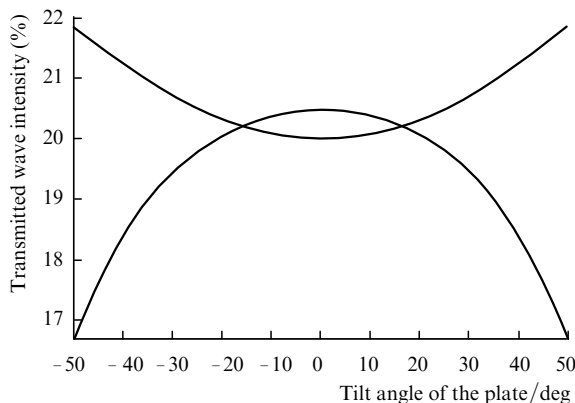

Figure 3. Dependences of the intensities of waves propagated through the polarisation filter on the tilt angle of the swinging birefringent plate.

We studied the effect of disbalance in the intensities of interfering waves on the ACF shape by constructing the autocorrelation function of a pulse with a Gaussian envelope:

$$f(t) = \int_{-\infty}^{+\infty} d\tau \left[g(t) + \sqrt{\xi}\, g(t+\tau) \right]^4,$$

$$g(t) = e^{-t^2/T^2} \cos\omega t,$$

(8)

where ξ is the ratio of the intensities of interfering waves; $g(t)$ is the time dependence of the field strength for a model Gaussian pulse of duration T; ω is the (mean) carrier frequency. Fig. 4 shows the autocorrelation function $f(t)$ with $\xi = 1.3$ and a ten-fold magnified modulus of the difference between independently normalised ACFs corresponding to the interference of waves with different and

equal intensities. The parameter $\xi = 1.3$ corresponds to the theoretical disbalance in the intensities of the pulse components for a calcite plate with a tilt angle $\Omega = 50°$. The theoretical value of the relative error in the measurement of the ACF of a pulse by an autocorrelator with calcite plates for $\Omega_{max} = 50°$, caused by the disbalance between the interfering waves, does not exceed 3 %.
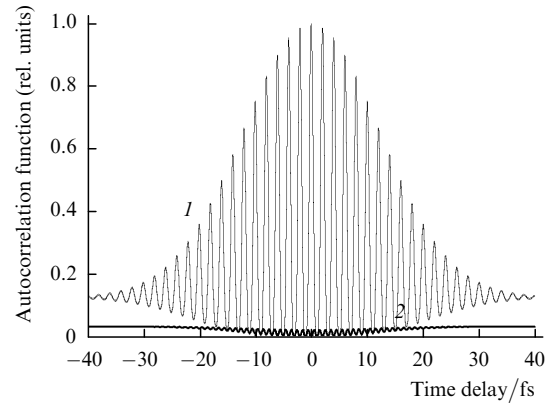

Figure 4. Theoretical ACF for unequal intensities of the radiation components ($\xi = 1.3$) (curve 1) and tenfold magnified modulus of the difference in independently normalised ACF corresponding to the interference of waves of different and equal intensities (curve 2).

The autocorrelator for experimental measurements was made of calcite plates of thickness 0.5 and 1 mm. The swinging of the 1mm-thick plate in the interval of angles $\pm\Omega = 15°$ was performed by an electromechanical drive with a DPR-52 dc motor. A film polariser was used as the polarising element of the autocorrelator. The autocorrelation function of the input pulses was obtained simply by making the radiation beam focused by a lens coincident with the working area of the nonlinear photodetector, no other adjustment of the autocorrelator being required. The optical elements of the autocorrelator did not have any coatings. The ACF could be recorded for an average power of 1 mW
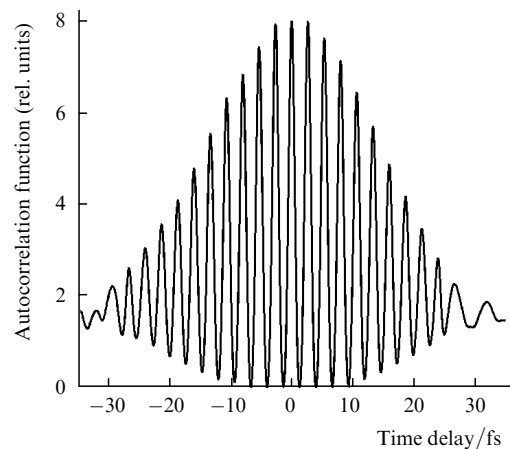

Figure 5. Experimental ACF of pulses emitted by a 'FEMoS' femtosecond Ti : sapphire laser (designed at the laser systems laboratory of the Novosibirsk State University). The FWHM of the ACF is 39 fs, and the pulse duration calculated assuming that the pulse envelope is described by the function sech^2 is 25 fs.

of the input radiation and a pulse repetition rate of 90 MHz. By using this autocorrelator, we obtained autocorrelation functions for the pulses generated by a femtosecond Ti : sapphire laser (Fig. 5). Assuming that the pulse envelope is described by the function sech^2, the measured laser pulse duration was 25 fs.

5. Conclusions

The use of a new scheme of a scanning interference autocorrelator for measuring the duration of ultrashort light pulses showed that if two birefringent plates of thickness 0.5 and 1 mm made of calcite, yttrium vanadate or rutile are employed, the scan range of the autocorrelator was about 180 fs at a wavelength of 800 nm when the swinging amplitude of the thicker plate was 15°. The optimal orientations of the optical axis of various crystals for attaining the maximum scan range are determined.

The disbalance in the intensities of pulse components, which is an inherent feature of the autocorrelator used in this work, was analysed numerically. This disbalance was found to affect the ACF shape only weakly.

Despite a comparatively small thickness of the bire-fringent plates used in the autocorrelator, the duration of ultrashort pulses propagating through them may increase due to dispersion spread. A detailed analysis of this effect for various input pulse durations in different spectral regions will be carried out in a separate publication. However, preliminary calculations of the dispersion spread lead to the conclusion that for a duration of transform-limited input pulses equal to or more than 20 fs, their dispersion spread in plates (for example, for an overall thickness 1.5 mm of calcite) does not exceed 10 % of their initial duration at a wavelength of 800 nm. In a longer-wavelength spectral region, the dispersion spread of the ultrashort-pulse components in autocorrelator plates decreases and achieves its minimum in the region of zero dispersion of their material (0.83 and 1.06 μm for calcite, 1.26 and 1.36 μm for yttrium vanadate, the first values corresponding to the ordinary wave and the second ones to the extraordinary wave).

References

1. Sarger L, Oberle J, in *Femtosecond Laser Pulses. Principles and Experiments* (Berlin: Springer-Verlag, 1998)
2. Diels J-C M, Fontaine J J, McMichael I C, Simoni F *Appl. Opt.* **24** 1270 (1985)
3. Yan C, Diels J-C M *J. Opt. Soc. Amer. B: Opt. Phys.* **8** 1259 (1991)
4. Kurobori T, Cho Y, Matsuo Y *Opt. Commun.* **40** 156 (1981)
5. Watanabe A, Tanaka S, Kobayashi H *Rev. Sci. Instr.* **56** 2259 (1985)
6. Watanabe A, Saito H, Ishida Y, Yajima T *Opt. Commun.* **69** 405 (1989)
7. Harde H, Burggraf H *Opt. Commun.* **38** 211 (1981)
8. Xinan G, Lambsdorff M, Kuhl J, Biachang W *Rev. Sci. Instr.* **59** 2088 (1988)
9. Yasa Z A, Amer N M *Opt. Commun.* **36** 406 (1981)
10. Baraulya V I, Kobtsev S M, Korablev A V, Kukarin S V, Yurkin A M *Techn. Progr. of IX Intern. Conf. 'Laser Optics'* (St. Petersburg, Russia, 1998), p. 79
11. Riffe D M, Sabbah A J *Rev. Sci. Instr.* **69** 3099 (1998)
12. Wang C L, Pan C L *Patent USA* No. 5 907 423 (1999)
13. Spielmann C, Xu L, Krausz F *Appl. Opt.* **36** 2523 (1997)
14. Reid D T, Padgett M, McGowan C, Sleat W E, Sibbet W *Opt. Lett.* **22** 233 (1997)
15. Reid D T, Sleat W E, Sibbet W *Patent USA* No. 6 195 167 (2001)
16. Kobtsev S M, Kukarin S V, Sorokin V B *Digest CLEO/Europe-2000* (Nice, France, 2000, CTuK 103), p. 138
17. Baraulya V I, Kobtsev S M, Korablev A V *Pis'ma Zh. Tekh. Fiz.* **24** (1) 62 (1998)
18. Reid D T, Sibbet W, Dudley J M, Barry L P, Thomsen B, Harvey J D *Appl. Opt.* **37** 8142 (1998)
19. Ranka J K, Gaeta A L, Baltuska A, Pshenichnikov M S, Wiersma D A *Opt. Lett.* **37** 8142 (1998)
20. Kikuchi K *Electron. Lett.* **34** 123 (1998)
21. Streltsov A M, Moll K D, Gaeta A L, Kung P, Walker D, Raze-ghi M *Appl. Phys. Lett.* **75** 3778 (1999)
22. Loza-Alvarez P, Sibbet W, Reid D T *Electron. Lett.* **36** 631 (2000)
23. Skovgaard P M, Mullane R J, Nikogosyan D N, McInerney J G *Opt. Commun.* **153** 78 (1998)
24. Rudolph W, Sheik-Bahae M, Bernstein A, Lester L F *Opt. Lett.* **22** 313 (1997)
25. Streltsov A M, Ranka J K, Gaeta A L *Opt. Lett.* **23** 798 (1998)
26. Landau L D, Lifshitz E M *Elektrodinamika Sploshnikh Sred* (Electrodynamics of Continuous Media) (Moscow: Nauka 1992), p.495
27. Kobtsev S M, Sventsitskaya N A *Opt. Spektrosk.* **73** 114 (1992)